31st International Conference
ENGINEERING MECHANICS 2025
Medlov, Czech Republic, May 12 –14, 2025
Paper **#25,** pp. 57–60, doi: 10.21495/em2025-57

FINITE ELEMENT ANALYSIS OF A MODULAR PIEZOELECTRIC MICROPUMP DESIGN

Ciganas J.[1], Cigane U.[2]

Abstract: *The growing interest in microelectromechanical systems (MEMS) technologies is driving research in this area. One of the important elements used in MEMS technologies are micropumps. Most often, micropumps have an integrated membrane made of different materials that is directly affected by the excitation source. In this work, the membrane is integrated into the housing (made of the same material) and is separated from the excitation source. This reduces the complexity of production and the number of parts to be assembled. Finite element analysis has shown that this type of micropump works and can achieve a performance of 1.25 µl/s. In addition, it is planned to improve the geometry, mathematical model, and manufacturing technology of the micropump to increase the micropump performance.*

Keywords: Micropump, Integrated membrane, Piezoceramic, Finite element analysis, MEMS technologies

1. Introduction

In recent years, scientists have conducted theoretical and experimental studies to design and develop microdevices, which has led to the advancement of microelectromechanical systems (MEMS) technologies (Iakovlev, Erofeev and Gorelkin, 2022; Ni et al., 2023). Piezoelectric micropumps have been found to be significant and have gained a lot of interest as microfluidic devices that can deliver fluids in small and precise amounts (Asadi Dereshgi, Dal and Yildiz, 2021; Li et al., 2021). Furthermore, micropumps have significant applications in the engineering and medical fields (Barua et al., 2021; Chappel and Dumont-Fillon, 2021; Chircov and Grumezescu, 2022; Luo, Yang and Cui, 2023).

The most common components used in micropumps are an actuator and a membrane, which are commonly assembled from different materials. In this paper, micropumps are developed using a simplified construction and operation method. Unlike typical micropumps, the micropump of the suggested design has a membrane that causes pressure variations within the chamber. The main difference is that the membrane is made from the same material as the housing rather than being constructed from a separate component or material. The vibrations of the actuator are transmitted through the housing, and because of the thinness of the membrane, it deforms more than the entire housing. The performance of the micropump was analysed using the finite element method using the software "COMSOL Multiphysics". The micropump is intended to be manufactured with a stereolithography (SLA) 3D printer. This type of micropump structure can be included into a microfluidic device or developed as a separate module.

2. Methods

2.1. Micropumps Geometry and Materials

The geometry of the proposed micropump was designed using the "COMSOL Multiphysics" software. The micropump model consisted of a housing, a piezoelectric ring, a membrane, a pump chamber, and inlet and outlet channels. The membrane was 0.5mm thick, and the diameter of the inlet and outlet channels was 1mm. To optimise the number of finite elements, the designed geometry was simplified to half the model.

[1] Assoc. Prof. Dr. Justas Ciganas: Faculty of Business and Technologies, Siauliai State Higher Education Institution; Ausros al. 40; 762 41, Siauliai; LT, j.ciganas@svako.lt

[2] Dr. Urte Cigane: Faculty of Business and Technologies, Siauliai State Higher Education Institution; Ausros al. 40; 762 41, Siauliai; LT, u.cigane@svako.lt

The geometry of the micropump is presented in Fig. 1(a). For the analysis, ultraviolet (UV) resin, lead zirconate, and water materials were selected. The mechanical characteristics of these materials are presented in Tab. 1.

Tab. 1: Mechanical characteristics of the materials

Materials	Properties	Value	Units
UV resin	Density	1130	kg/m^3
	Tensile strength	40-50	MPa
	Poisson‘s ratio	0.45	-
Lead Zirconate	Density	7500	kg/m^3
	Coupling coefficient (k_{33})	0.75	-
	Displacement coefficient (d_{33})	$650 \cdot 10^{-12}$	m/V
	Voltage coefficient (g_{33})	$19 \cdot 10^{-3}$	V·m/N
Water	Density	997	kg/m^3
	Dynamic viscosity	0.001	Pa·s

2.2. Finite Element Model

The designed model was further decomposed into finite elements using free quad and tetrahedral elements. To increase accuracy, a mess refinement was performed around the chamber and channels. Additionally, a grid-independent verification study was performed. The final finite element model is presented in Fig. 1(b).

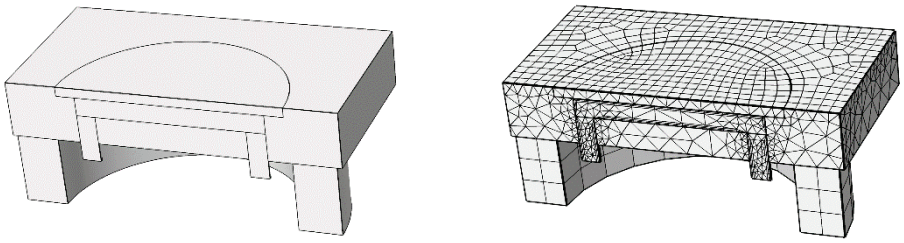

(a) (b)

Fig. 1: Micropump design: (a) 3D model; (b) finite element model.

The resulting finite element model consisted of 10 515 domain elements, 2 987 boundary elements, and 603 edge elements.

2.3. Algorithm and Boundary Conditions

This finite element analysis included three physics (solid mechanics, electrostatics physics, and laminar flow), which were combined into two Multiphysics (piezoelectric effect and fluid - structure interaction) tasks. The deformation of the piezoceramic was solved in the first Multiphysics task. The question of how the membrane deformations determine the fluid flow behaviour was solved in the second Multiphysics task. Boundary conditions were also used in the model. In the solid mechanics physics part, symmetry and fixed constraint boundary conditions were used. The symmetry condition was reproduced by a simplified geometry since it was determined that the remaining part would deform identically to the calculated one. The lower part of the piezoceramic was established as a fixed constraint.

In the Electrostatics physics section, the terminal and ground boundary were used. The main parameter of the terminal boundary condition was the voltage. The voltage could be described by the following equation:

$$V = V_0 \cdot sin\,(t \cdot f \cdot 2 \cdot \pi) \cdot R(t \cdot f \cdot 4/3) \tag{1}$$

where V_0 is the applied voltage, t is the time, f is the piezoceramic frequency, and R is a ramp function.

The terminal boundary condition was marked on the upper part of the piezoceramics. The ground boundary condition was marked, as well as the reinforcement part (lower part of the ceramics).

The Laminar Flow Physics Section described the fluid parameters. The left channel was labelled as inlet and the right as outlet. To create a flow in a micropump, there must be valves that allow the flow in one

direction. In full geometry, this could be a Tesla valve, thermopneumatic valve, magnetic-actuated microvalve, etc. (Qian et al., 2020). In this analysis, the inlet channel was described by the if condition:

$$p_0 = if(av_{in}(w_2) > 0, -low_{stress}, high_{stress}) \cdot (av_{in}(w_2)^2, av_{in}(\rho)) \quad (2)$$

where p_0 is the pressure, av_{in} is the average value of the flow, w_2 is the flow direction along the z-axis, and ρ is the density of the fluid.

The contact walls with the fluid and the shell were marked as wall boundaries.

3. Results and Discussion

After performing a finite element analysis, the image of the deformation and the accumulated flow volume vs. time graph were obtained. These results confirmed the operating principle of the micropump of the designed geometry and predicted the main characteristics of the micropump. The results are presented in Fig. 2.

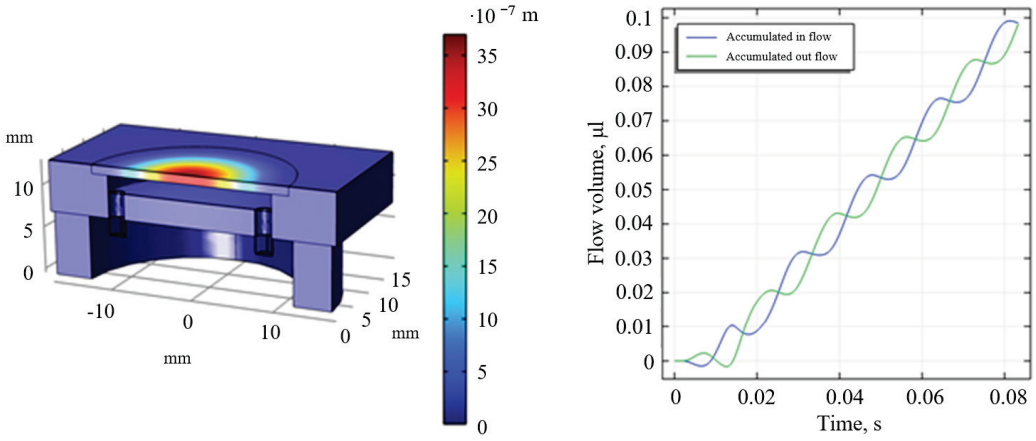

(a) (b)

Fig. 2: Results of finite element analysis: (a) deformations of the membrane; (b) graph of accumulated flow volume vs. time.

Membrane deformation studies showed that the maximum membrane deformation was achieved using a frequency of 60 Hz. In the Fig. 2, it can be seen that at a frequency of 60 Hz, the central part of the membrane deformed sinusoidally up to 3.5 µm. Such a deformation allowed pressure differences in the chamber. As a result of different channel conditions, the liquid started to flow through the micropump.

The accumulated flow volume vs. time graph presented two curves - accumulated in flow and accumulated out flow. The graph showed that due to the pressure difference created by the membrane, the accumulated flow volume was constantly increasing. With different membrane deformation and suction cycles, the liquid flowed through one channel as the membrane bent outward, while a small amount of liquid returned through the other channel. However, the amount of liquid that flowed in significantly exceeded the amount that returned. A similar cycle continued as the membrane bent inward, but at that time, the liquid flowed more intensively through the outflow channel. The efficiency of the micropump was found to be 1.25 µl/s.

This prototype design of the micropump will be improved by varying different geometric parameters, materials, and excitation parameters. In this work, the equation that defined the operation of microvalves was used for calculations, but with different valve types, it is necessary to analyse their influence on the performance. Therefore, valve models and their analysis should be included in further modelling.

4. Conclusion

This work presents a micropump design with a simplified manufacturing method. The finite element analysis in "COMSOL Multiphysics" software showed that the membrane movement caused by the piezoelectric ring creates a pressure difference that drives the fluid to flow through the micropump. Analysis revealed that maximum membrane deformation at an excitation frequency of 60 Hz reaches 3.5 µm. This deformation creates a pressure difference that drives the fluid to flow through the inlet and outlet channels. The resulting micropump efficiency is 1.25 µl/s. This study contributes to the development and

advancement of micropumps. In the future, it is planned to improve this technology by varying the geometric parameters, materials, and excitation conditions. Experimental studies will also be conducted to confirm the modelling results and evaluate the practical operation of the micropump.

References

Asadi Dereshgi, H., Dal, H. and Yildiz, M.Z. (2021) Piezoelectric micropumps: state of the art review. *Microsystem Technologies*, 27, pp. 4127–4155.

Barua, R., Datta, S., Sengupta, P., Chowdhury, A.R. and Datta, P. (2021) Chapter 14 - Advances in MEMS micropumps and their emerging drug delivery and biomedical applications. In *Advances and Challenges in Pharmaceutical Technology.* Eds: Nayak, A.K., Pal, K., Banerjee, I., Maji, S. and Nanda, U. Elsevier, Amsterdam.

Chappel, E. and Dumont-Fillon, D. (2021) Chapter 3 - Micropumps for drug delivery. In *Drug Delivery Devices and Therapeutic Systems*. Ed.: Chappel, E. Elsevier, Amsterdam.

Chircov, C. and Grumezescu, A.M. (2022) Microelectromechanical Systems (MEMS) for Biomedical Applications. *Micromachines*, 13, 164.

Iakovlev, A.P., Erofeev, A.S. and Gorelkin, P.V. (2022) Novel Pumping Methods for Microfluidic Devices: A Comprehensive Review. *Biosensors*, 12, 956.

Li, H., Liu, J., Li, K. and Liu, Y. (2021) A review of recent studies on piezoelectric pumps and their applications. *Mechanical Systems and Signal Processing*, 151, 107393.

Luo, X., Yang, L. and Cui, Y. (2023) Micropumps: Mechanisms, fabrication, and biomedical applications. *Sensors and Actuators A: Physical*, 363, 114732.

Ni, J., Xuan, W., Li, Y., Chen, J., Li, W., Cao, Z., Dong, S., Jin, H., Sun, L. and Luo, J. (2023) Analytical and experimental study of a valveless piezoelectric micropump with high flowrate and pressure load. *Microsystems & Nanoengineering,* 9, 72.

Qian, J.-Y., Hou, C.-W., Li, X.-J. and Jin, Z.-J. (2020) Actuation Mechanism of Microvalves: A Review. *Micromachines*, 11, 172.